THESIS FOR THE DEGREE OF LICENTIATE OF ENGINEERING

in Thermo and Fluid Dynamics

The effects of long chain alcohol blends on engine performance and spray characteristics in CI engines

JOSEFINE PREUß

Division of Combustion and Propulsion Systems
Department of Mechanics and Maritime Sciences
CHALMERS UNIVERSITY OF TECHNOLOGY
Göteborg, Sweden 2018

The effects of long chain alcohol blends on engine performance and spray characteristics in CI engines

Josefine Preuß

THESIS FOR THE DEGREE OF LICENTIATE OF ENGINEERING
no 2018:26

Department of Mechanics and Maritime Sciences
Division of Combustion and Propulsion Systems
Chalmers University of Technology
SE-412 96 Göteborg, Sweden
Phone: +46 (0)31-772 10 00

Author e-mail: preuss@chalmers.se

Chalmers Reproservice
Göteborg, 2018

Abstract

Replacing fossil fuels with alternatives derived from renewable sources is one way of meeting society's increasing need for mobility while also significantly reducing greenhouse gas emissions from vehicles with internal combustion engines. To facilitate such a replacement, this thesis presents engine experiments and optical spray studies conducted to evaluate the potential of blends of biomass-derived alcohols and vegetable oils to serve as drop-in fuels for compression ignition engines. A drop-in fuel is a fuel whose properties match those of fossil Diesel closely enough to allow its use in unmodified conventional Diesel engines without any adjustment of their calibration settings. Two C_8-alcohols (n-octanol and its isomer 2-ethylhexanol) and two C_{10}-alcohols (n-decanol and its isomer 2-propylheptanol) were blended with hydrotreated vegetable oil (HVO) and rapeseed methyl ester (RME) or fossil Diesel. The percentage of fossil Diesel in the blends was 0%, 10% or 20%. Blends without any Diesel contained 7% RME. The impact of blend composition on the performance and emissions of a Volvo D13 single cylinder heavy duty research engine operated with standard settings was then investigated by considering four load points adapted from the European Stationary Cycle. To complement the engine studies, the spray characteristics of selected blends of 2-ethylhexanol and HVO with either 20% Diesel or 7% RME were investigated in a high-pressure/high-temperature chamber. Optical experiments were performed under non-combusting and combusting conditions at injection pressures of 120 and 180 MPa, respectively.

The engine experiments revealed that the performance with the studied blends was comparable to that achieved with standard Diesel in terms of the indicated thermal efficiency. Because of the blends' lower heating value, they yielded slightly lower indicated mean effective pressures than conventional Diesel, leading to increased specific fuel consumption. The yields of HC and NOx achieved with the blends did not differ significantly from those seen with Diesel. However, the blends produced less carbon monoxide and significantly less soot. Fully renewable blends with RME and no fossil Diesel produced the lowest soot emissions because they had the highest oxygen content and contain no aromatic compounds, which are known soot precursors. Particle size distribution analyses showed that standard Diesel contained considerably more particles with diameters above 23 nm than the blends. The blends thus yielded large numbers of small soot particles (> 23nm) and a higher total number of particles than Diesel. Several optical methods were used to characterize the combustion process. Shadow imaging under non-combusting conditions was used to measure the blends' liquid and vapor penetration lengths. The HVO and EH blends exhibited greater liquid penetration lengths than the other tested fuels, but all fuels exhibited similar vapor penetration. Under combusting conditions, the lift-off length, ignition delay,

start of soot formation, and soot volume fraction were measured by simultaneously recording time-resolved two-dimensional laser extinction, flame luminosity and OH*chemiluminescence images. All tested fuels had similar liquid penetration lengths. Despite their different CNs, Diesel and HVO had similar ignition delays. Conversely, the EH blends had longer ignition delays than Diesel despite having the same CN. The ignition delay must thus depend on other parameters such as the latent heat of evaporation. The lift-off length was found to be highest for the blend with the highest content of EH. In accordance with the engine experiments, the blends yielded a lower soot volume fraction than conventional Diesel.
Overall, the obtained results indicate that blends based mainly on long-chain alcohols could be viable replacements for fossil Diesel fuel.

List of publications

This thesis is based on the following publications:

I. J. Preuß, K. Munch, I. Denbratt, "Performance and emissions of long-chain alcohols as drop-in fuels for heavy duty compression ignition engines," *Fuel*, vol. 216, pp. 890–897, 2018

II. J. Preuß, K. Munch, M. Andersson, I. Denbratt, "Comparison of long-chain alcohol blends, HVO and Diesel on spray characteristics, ignition and soot formation," *SAE Technical Paper 2019-01-0018*, 2019.

Acknowledgement

First I like to thank my supervisors Ingemar Denbratt and Karin Munch for the opportunity to work in this exciting project. Thank you Ingemar for the fruitful discussions and your support, whenever I needed it. And thank you Karin for the the good exchange of ideas, the motivation you give me and the good working atmosphere you create.
This work is part of the project 'Future alternative transportation fuels' funded by the Swedish Energy Agency, which I thank for the financial support.

I am grateful for the help I got in with my experimental work from the lab engineers especially from Timothy Benham, Alf-Hugo Magnusson, Patrik Wåhlin and Lars Jernqvist. Thank you for sharing your expertise with me.
The help with the spray chamber tests from Chengjun Du and Mats Andersson was highly appreciated. Thank you Mats for patiently answering all my questions and Chengjun for guiding me through the optical set-up.

The project involves many people and I consider myself lucky that the work atmosphere is very adjuvant, productive and friendly. Thank you Maria Grahn, Nika Alemahdi, Sofia Poulikidou, Stefan Heyne and Tara Larsson. Also I am thanking Ulf Östan from Saybold for the support with the CN tests. Further I like to acknowledge Lisa Jacobsson-Nilsson, Arjan Helmantel, Fredrik Ekström and Håkan Persson amongst others from Volvo Cars for their support with the engine tests.

That I have so helpful and funny colleagues at the division, makes my work enjoyable. I like to especially thank Elenor Norberg, Ulla Lindberg-Thieme, Erik Sjödin and Sven Andersson. As well as former colleagues.

At last, I like to thank my parents for their support, my sambo Anders and my daughter Frida for bringing me joy every day.

Contents

List of Figures

List of Tables

1 Introduction

1.1 Motivation

Because of the anthropogenic greenhouse effect and global warming, there is an urgent need to transition away from a fossil fuel-based economy to one that is more sustainable. In 2015, The transport sector accounted for 24% of the world's total greenhouse gas emissions, primarily because of its CO_2 output. Three quarters of these emissions originated from road traffic. In 2016, around half of the vehicles operating in the European Union (the EU-28) were powered by a compression ignition (CI) engine. CI engines are efficient and robust, and are therefore preferred for heavy duty vehicles. Most of the remaining vehicles are powered by gasoline engines, but there is also a small but growing proportion of hybrid, plug-in hybrid, and fully electric vehicles. Statistics compiled by the European Environmental Agency show that emissions from road transport decreased between 1990 and 2015. However, the decline was smaller than expected due to increasing mobility and the high proportion of CI engines using fossil Diesel fuel [1]. Emissions from road traffic have strong negative effects on air quality, especially in urban areas, and cause several health and environmental problems. Engine exhaust contains several pollutants, including nitrogen oxides (NOx), carbon monoxide (CO), methane, and volatile organic compounds that contribute to ozone formation in the atmosphere, leading to adverse climatic effects. The release of NOx, sulfur oxides, and ammonia into the atmosphere causes the acidification of soils and waters. Most modern Diesel fuels therefore have a very low sulfur content or are sulfur-free. Particulate matter emissions from internal combustion engines also have negative effects on human health; in particular, they are linked to many respiratory problems [2]. To control the risks presented by exhaust emissions and to reduce the danger they present to public health, many jurisdictions have introduced laws requiring vehicle manufacturers to reduce the emissions of their products. Table 1 shows the current emissions standards for Europe, the United States, Japan, and China. Stricter emissions regulations are expected in the near future.

Since 2013 in the EU and 2018 in China, these regulations have included limitations on particle number emissions. Measures introduced to reduce the environmental impact of fossil fuels (e.g. by reducing their contents of sulfur and aromatics) and the introduction of alternative fuels (in the form of fuel blends) changes the nature of the particulate matter in the exhaust. Procedures for capturing particles are based on the Particle Measurement Programme (PMP), which establishes standard particle size distribution measurement and analysis methods. A particle size of 23 nm was set as the cut-off size for particle number counting, mainly due to restrictions in measurement technology [4]. However, technological advancements have made it possible to detect and

Table 1.1: Latest emissions standard for Europe, the U.S, Japan and China [3]

Emission Standard	Area	Driving cycle	year	CO	HC	NOx	PM	PN	NH3
				g/kWh				1/kWh	ppm
EURO VI	EU	WHSC	2013	1,5	0,13	0,4	0,1	$8{,}0 * 10^{11}$	
U.S. EPA & California	U.S.		2015	20,8	0,19	0,27	0,01		
Japan	Japan	WHTC	2016	2,2	0,17	0,4	0,01		
China VI CI	China	WHSC	2018	1,5	0,13	0,4	0,01	$8{,}0 * 10^{11}$	10
		WHTC	2018	4	0,16	0,46	0,01	$6{,}0 * 10^{11}$	10

count smaller particles reliably, so a decrease in the cut-off size is likely in the future. One way to achieve compliance with these new legal emissions standards is to introduce fuels produced in a sustainable fashion. The use of oxygenated alternative fuels (e.g. alcohols and fatty acid esters) could make it possible to reduce emissions of CO_2, CO, and soot while maintaining engine performance [5, 6, 7, 8]. Several renewable alternative fuels for compression ignition engines are commercially available. Fuels containing Biodiesel, which consists mainly of fatty acid esters produced by the transesterification of vegetable oils together with fossil Diesel are referred to as 'BXX', where 'XX is a two-digit number representing the proportion of biodiesel in the blend. Blends containing up to 20% biodiesel (B20) can be used in standard engines but their use generally voids the manufacturer's warranty on the vehicle. Modified engines are usually required to enable the use of pure biodiesel (B100). In some countries, fossil Diesel is routinely blended with up to 7% rapeseed methyl ester (RME).

1.2 Objective

This work aims to identify potential alternative fuels that could be used in compression ignition engines in the near future. Specifically, the objective was to identify fuels that can be produced renewably and can be used as drop-in replacements for fossil Diesel, meaning that they can be used in existing Diesel engines without requiring any changes in the engines' hardware or engine calibration. In addition, drop-in fuels must be compatible with the materials used in existing engines, achieve cold starts without issue, and be compatible with established fuel distribution infrastructure. A preliminary screen of candidate fuels was conducted, focusing on blends featuring the C_8- alcohols n-octanol (Oc) and its isomer 2- ethylhexanol (EH) and the C_{10}-alcohols n-decanol and its isomer 2-propylheptanol (PH). These alcohols were blended with hydrotreated vegetable oil (HVO) and Diesel or RME. Because they have eight- or ten-atom carbon chains, the

studied alcohols are referred to as long-chain alcohols (as compared to short-chain alcohols such as ethanol, which has a carbon chain length of two). The impact of blend composition on engine performance and emissions was studied experimentally using a Volvo D13 single cylinder heavy duty research engine, which was operated using its standard settings. Deeper insights into the combustion behavior of selected fuel blends were obtained by performing optical experiments in a constant volume high-pressure/high-temperature chamber.

2 Theoretical background

This chapter begins by discussing the properties, production, and usage of selected renewable fuels including hydrotreated vegetable oil, rapeseed methyl ester, the C_8-alcohols n-octanol and its isomer 2-ethylhexanol, and the C_{10}-alcohols n-decanol and its isomer 2-propylheptanol. Isomers are substances with the same stoichiometric formula but different structures. Because of their structural differences, their chemical and physical properties differ, as does the complexity of their production. After discussing the fuels, the current state of research on alternative fuels is outlined. Finally, because the project's objective is to identify fuels suitable for use in compression ignition (CI) engines, the operating principles of CI engines are introduced along with a conceptual model of a Diesel jet and a discussion of exhaust emissions.

2.1 Fuel properties

Some key properties of the individual components of the studied fuel blends are presented in Table 2.1, along with the properties required for compliance with the EN 590 standard and the properties of fossil Diesel. The EN 590 standard defines the physical properties a fuel must possess to be sold in the EU and some other European countries.

n-Octanol is used as synthetic intermediate in the production of surfactants, perfumes and flavors. It can be prepared from fossil resources via the reaction of butadiene with water [15]. However, it has also been produced renewably on a lab scale via biosynthesis using the bacterium *Escherichia coli* [16, 17]. In addition, Julis and Leitner [18] demonstrated the production of n-octanol by the conversion of biomass-derived furfural and acetone. ***2-Ethylhexanol*** be produced from fossil propene via a multi-step catalytic process involving reactions with CO_2 and hydrogen [19], or via the Guerbet reaction of n-butanol [20]. It could also plausibly be produced from renewable ethanol.

n-Decanol is used as plasticizer, lubricant, and surfactant, and can be biosynthesized in *E. coli* in a manner similar to n-octanol. ***2-Propylheptanol*** is used as a plasticizer in the production of polyvinyl chloride and other materials, and also as a surfactant or synthetic lubricant. Its production processes are similar to those of 2-ethylhexanol.

The C_8- and C_{10}-alcohols have Diesel-like densities and boiling points at the lower end of the accepted range for Diesel. They all have lower CN values than Diesel, and because of their branched structures, EH and PH have lower CN values than their linear isomers. However, all long-chain alcohols have higher CNs than the short chain alcohols methanol and ethanol. Moreover, their lower heating values (LHV) are higher than those of the commercially used fuel ethanol

Table 2.1: Fuel properties [9, 10, 11, 12, 13, 14**?**]

		EN590	**Diesel**	**n-Octanol**	**2-Ethyl-hexanol**	**n-Decanol**	**2-Propyl-heptanol**	**HVO**	**RME**
				$C_8H_{18}O$	$C_8H_{18}O$	$C_{10}H_{22}O$	$C_{10}H_{22}O$	$C_{13.3}H_{28.5}$	$C_{21}H_{38}O_2$
Density	kg/m^3	820-845	830	830	832	829	832	779.9	883
CN		51	52	37.5	23.2	48.2	33.3	87.8	52
Flash point	$^\circ C$	> 55	> 55	80	75	> 80	100	94	120
Calorific value	MJ/kg		42.9	38.4	38.4	38.9	38.9	44.1	38
Oxygen content	%	-	-	12.3	12.3	10.3	10.3	-	10
Boiling point	$^\circ C$	180-370	150-370	195	184	221.5	218	180-320	317
Viscosity Kin. 40$^\circ C$	mm^2/s		<4.5	5.5	5.2	8.3	17.7 ($20^\circ C$)	2.6	4.5
Latent heat of evaporation	kJ/kg		250	545	389	310			
Vapor pressure (25$^\circ C$)	mbar		<1.2	0.13	0.266	0.01	0.21	0.09	
Molar weight	g/mol		167.3	130.2	130.2	158.3	158.3	187.9	322.5
H/C			1.92	2.25	2.25	2.2	2.2	2.15	1.81
O/C			-	0.125	0.125	0.1	0.1	-	0.095

(26.8 MJ/kg) [21]. The energy output per kilogram of fuel increases with the carbon chain length. However, the longer the chain length, the lower the molar percentage of oxygen. The latent heat of evaporation is a measure of the amount of energy needed to induce the fuel to go from the liquid to the gaseous state. The alcohols have a higher heat of evaporation than Diesel. They also have higher kinematic viscosities, which can cause problems during fuel injection and spray formation.

Hydrotreated vegetable oil is an aliphatic paraffinic hydrocarbon with properties similar to Diesel fuel. It can be produced from a wide range of feedstocks, all of which yield products of similar quality. The feedstock for the HVO used in Sweden consists mainly of oil from vegetable or animal waste (38%), slaughterhouse waste (19%), and palm fatty acid distillate (23%). In recent years, the use of HVO has increased markedly. Palm oil has not been used as a feedstock for its production since 2016, however its distillate has become an increasingly important feedstock. Elsewhere in the world, it is commonly produced from soy bean oil. Other possible feedstocks include rapeseed, sunflower, or palm oil, as well as jatropha and algal oil [22]. HVO production involves an initial pretreatment process that removes impurities from the feedstock. The unsaturated fatty acid chains are then converted to less reactive oxygen-free saturated paraffinic alkanes via a two-stage hydrotreatment and isomerization process. Depending on the feedstock, the car-

bon chain length of HVO ranges from C_{15}-C_{18} [13]. HVO has the benefit of a high heating value and high CN (>70), is sulfur-free, and has a low aromatic content (< 1% by mass). Its density is slightly lower than that of standard European Diesel fuel, and outside the range permitted by the EN590 standard. However, its high heating value compensates for its low density. Its boiling point is lower than that of Diesel, and its boiling curve is less steep. Consequently, it can be used at temperatures as low as – $40°C$ [13].

Rapeseed methyl ester contains saturated and unsaturated fatty acids. It is produced by extracting rapeseed oil, refining it, and then subjecting it to transesterification. Its properties are similar to those of Diesel, although its density is slightly higher. It has already been integrated into the existing transportation fuel infrastructure and is blended with fossil Diesel (at levels of up to 7% by mass in some EU countries) to reduce well-to-wheel CO_2, CO, HC and particulate emissions. Its effects on NOx emissions depend on the engine design and manufacturer [23, 24, 25].

All of the fuel components considered in this work have flash temperatures above $55°C$ and so are class 3 fuels. In addition, they are all immiscible with water and have low susceptibility to microbial growth, enabling long-term storage.

2.2 The state of the art in alternative fuel research

Several researchers have shown that adding alcohols to standard Diesel fuel can help reduce NOx and soot emissions. The reduction in soot emissions can be partly attributed to the blended fuel's higher oxygen content [5, 21, 26, 27, 28, 29]. The production of ethanol is increasing, and many researchers have investigated its use as a fuel or a component of blended fuels with fossil Diesel or gasoline (e.g. [5, 28, 30]). The key disadvantage of short chain alcohols such as ethanol is their low heating value. Longer chain alcohols avoid this deficiency because the heating value increases with the carbon chain length. However, the longer the carbon chain, the lower the oxygen content of the blend.

Blends of fossil Diesel and longer chain alcohols such as butanol or pentanol have also been studied, revealing that they achieve performance comparable to that of conventional Diesel with the benefit of reduced emissions due to their alcohol content [31, 32, 33]. Only a few publications have examined blends using n-octanol or other alcohols with longer chains. Heuser et al. [7] tested neat n-octanol as a fuel in a single cylinder research engine, revealing that it produced similar NOx emissions to Diesel, higher HC and CO emissions, and significantly lower particulate emissions. Moreover, the engine's indicated efficiency was similar to that achieved with Diesel. These results were confirmed by optical experiments using n-octanol in a high pressure chamber and 1D simulations [34]. Zhang et al. [29] evaluated the performance of a blend containing 30% 2-ethylhexanol in Diesel. Compared to conventional Diesel, this blend reduced particulate

emissions and CO but slightly increased HC emissions at higher loads and had no effect on NOx emissions. Janssen et al. [27] investigated the potential of n-decanol in a single cylinder research engine with EGR and found that it yielded 90% lower particulate emissions than Diesel. 3D-CFD simulations supported this conclusion, indicating that the higher heat of evaporation of n-decanol led to locally reduced temperatures in the reaction zone and thus lower soot formation. Moreover, soot was oxidized earlier in the combustion process when using the alcohol.

Interest in HVO has increased in recent years because of its Diesel-like properties which allow it to be blended with Diesel and used in most existing CI engines. Aatola et al. [35] and Hartikka et al. [36] found that both neat HVO and a blend containing 30% HVO in Diesel yielded lower emissions of CO, HC, NOx and soot compared to neat Diesel when burned in a heavy duty DI engine with default injection timing settings. If the operating conditions were adjusted to maintain constant NOx emissions, the HVO-containing fuels yielded even lower emissions and a lower specific fuel consumption. In addition, HVO-containing blends do not clog engines' aftertreatment systems, and their spray characteristics (penetration length, droplet size, and spray cone angle) closely resemble those of fossil Diesel. Lapuerta et al. [37] tested blends of HVO and ultra-low sulfur Diesel with HVO contents ranging from 10-75%, and found that the main factor limiting the usable percentage of HVO was its low lubricity. It was therefore recommended that the HVO content of HVO-Diesel blends should be capped at 50%. However, several car manufacturers permit the use of neat HVO with added lubrication in their engines.

2.3 Compression ignition engine

Compression engines are more efficient than spark ignition engines, mainly because they can use higher compression ratios. This section presents a conceptual model of Diesel combustion and discusses the gaseous and particulate emissions produced by Diesel engines.

2.3.1 Conceptual model of a reacting Diesel jet

To help understand Diesel combustion, a conceptual model of a burning Diesel fuel jet under quasi steady state conditions was developed by Dec [38] on the basis of data from optical experiments. As shown in Figure 1, the behavior of injected liquid fuel leaving the nozzle is discribed. As hot air is entrained into the jet of liquid fuel, the fuel is vaporized, forming a rich fuel-air mixture close to the tip of the liquid spray. In this region, where the equivalence ratio is 3-5 and temperatures are above 1600 K, soot formation is initiated by polycyclic aromatic hydrocarbons (PAH), which are known to be key soot precursors. Final oxidation of soot takes place in the diffusion flame on the periphery of the jet, and NO forms in the lean regions of the diffusion flame.

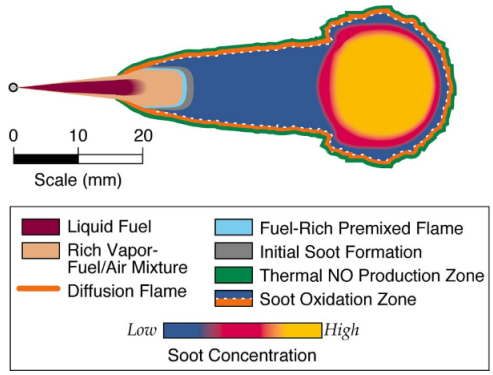

Figure 2.1: Conceptual model of Diesel combustion [38]

Other models, such as that developed by Kosaka et al. [39], also account for soot formation in the fuel-rich region. These models predict that soot particles coagulate and thus increase in size as they move downstream. Head vortices then move soot particles from the spray tip to the spray periphery, where they are oxidized. In contrast to Dec's model, this model suggests that the liquid penetration length should exceed the lift-off length.

2.3.2 Exhaust gas emissions

Carbon monoxide is formed as a result of incomplete combustion and thus incomplete fuel oxidation. Therefore, CO emissions depend on the air-fuel ratio. CI engines usually operate under lean conditions (lambda > 1) and are therefore expected to produce low CO emissions.
Hydrocarbon emissions consist of fuel that has not been burned as a result of overmixing or undermixing. Problems with fuel injection (such as nozzle sac leakage and injector needle bounce) can also cause a high concentration of unburned hydrocarbons.
Nitrogen oxides (NOx) are formed by high-temperature reactions between nitrogen and oxygen during combustion. The term NOx refers to nitrogen oxide (NO) and nitrogen dioxide (NO_2). Higher flame temperatures during combustion are directly related to higher NOx emissions.

2.3.3 Particle emissions

Particles can be classified as coarse mode particles with diameters above 20 nm, accumulation mode particles with diameters of 20-500 nm, and nucleation mode particles with diameters of 3-30 nm. Accumulation mode particles consist mainly of carbonaceous agglomerated and absorbed material, while nucleation mode particles consist of volatile organic and sulfur compounds.

Nucleation mode particles account for only 10% of the total particle mass emitted by CI engines but 90% of the total particle number. Therefore, accumulation and coarse mode particles account for the majority of the mass of particulate emissions. Figure 2 shows a typical exhaust particle size distribution [40].

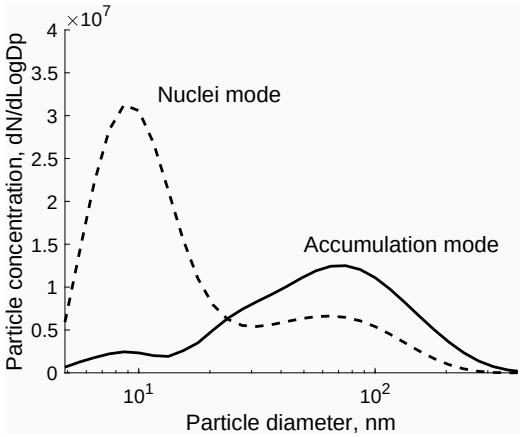

Figure 2.2: Typical exhaust particle size distribution (adapted from [40])

In accordance with Dec's conceptual model, soot formation is initiated by PAH in the fuel-rich premixed region downstream of the liquid spray. During the early stage of particle formation, precursor molecules coagulate into larger primary particles, which then agglomerate. Smaller particles are likely to sinter on the resulting agglomerated particles. The extent of agglomeration to bigger particles depends on the number of precursors (aromatic structures) that are present. After the exhaust leaves the tailpipe, the formation of nucleation mode particles will depend on the concentration of residual accumulation mode particles, the dilution, and the temperature. Rapid cooling and a low initial concentration of precursors (and thus soot) favor nucleation mode particles, whereas a high initial concentration of agglomerated particles favors the adsorption of particles onto existing ones [41].

3 Experimental equipment and methods

3.1 Fuel blending strategy

To facilitate their use as drop in fuels, the studied fuel blends were designed to have properties closely resembling those of fossil Diesel, particularly in terms of their CN. Alcohols have relatively low CN values, which can be compensated for by the relatively high CN of HVO (see Table 2.1). The Diesel content of the blends was set to 0%, 10%, or 20% by volume, blends with no Diesel had an RME content of 7%. The content of HVO was capped at 50%. The CN of n-decanol was found to be high enough to not require blending. The compositions of the studied blends are shown in Table 3.1, together with their oxygen contents (Ox), densities, LHVs, and CNs. The CNs were determined according to EN ISO 5165. To guarantee smooth injection, a lubricant was added to the alcohol components at a concentration of 200 ppm before blending. The blends were named based on the abbreviations of their constituents and their volumetric percentage in the blend.

Table 3.1: Fuel blend characteristics

	Fuel	**Diesel**	**HVO**	**RME**	**Ox**	**Density**	**LHV**	**CN**
	vol.%	vol.%	vol.%	vol.%	m.%	kg/m^3	MJ/kg	-
Reference		100	-	-	-	830	43.16	52
Oc	47	20	33	-	5.8	813.5	41.12	52
	55	10	35	-	6.8	812.5	40.77	51.2
	58	-	35	7	7.8	816.2	40.28	49
EH	36	20	44	-	4.4	808.7	41.74	51.9
	45	10	45	-	5.5	808.4	41.34	52.3
	43	-	50	7	6	809.5	41.12	52.1
PH	46	20	34	-	4.6	813.9	41.41	52.4
	55	10	35	-	5.6	813.6	41.05	50.9
	58	-	35	7	7.8	817.3	40.57	49.3
Dec	100	-	-	-	10.3	829	38.9	48.2

3.2 Heavy duty CI engine

Experiments were performed on a heavy duty compression ignition single cylinder research engine with a compression ratio of 17:1 and a cylinder head from a Volvo D13 engine. Table 3.2 shows the detailed engine specification.

Table 3.2: Heavy duty CI engine specifications

Engine	AVL 501 single cylinder
Cylinder head type	Volvo D13
Displaced volume	2130 cm3
Bore	131 mm
Stroke	158 mm
Connecting rod length	267.5 mm
Compression ratio	17:01
Number of Valves	4
Fuel injection System	Common rail
Number of nozzles holes	5

Four load points adapted from the European Stationary Cycle (ESC) were used: A25, B50, B75 and C75. Here, B50 was deployed as a reference point, which was run at the beginning and end of each test cycle to evaluate the change in engine performance over time. Table 3.3 lists the engine parameters adapted from the factory settings. To investigate the influence of the fuel on combustion characteristics and emissions, all engine parameters were kept constant for all fuel blends as well as the Diesel reference.
The fuel consumption was measured with an AVL 733S fuel balance, and a Delphi common rail F2 injector was used to inject fuel into the combustion chamber. A pressure sensor (Kistler 7061B) and piezo amplifier (Kistler 3066A01) were used to record cylinder pressure traces, which were sampled with Osiris data acquisition software at a resolution of 0.1 CAD. The engine was equipped with an AVL554 oil cooling unit and AVL553 water cooling unit. Exhaust gas recirculation (EGR) was regulated with a valve in the exhaust pipe. The EGR value was calculated as the quotient of A and B, where A is the CO_2 content of the intake air minus that of the ambient air, and B is the CO_2 content of the exhaust air minus that of the ambient air.

3.2.1 Analytical devices

Exhaust gas emissions were detected using an AVL AMA i60 iGEM emission measurement system. Nitrogen oxides were measured with a chemiluminescence system, which detects light emit-

Table 3.3: Engine operating conditions

Operating conditions	Unit	A25	B50	B75	C75
Speed	r/min	1200	1500	1500	1800
Torque (Diesel)	Nm	85	160	239	209
IMEP (Diesel)	bar	6.1	11.0	15.9	14.1
Inj. time	BTDC	4.52	7.8	9.4	4.5
Inj. duration	μs	668	1060	1466	1346
	CAD	4.8	9.5	13.2	14.5
Inj. pressure	bar	1800	1800	1800	1800
EGR	%	16.5	12.9	12.5	17.5
Boost pressure	mbar	1260	1936	2457	2726
Fuel flow	kg/h	2.39	5.14	7.37	8.17

ted during the reaction of nitrogen in the sample with ozone; the concentration of nitrogen oxides is proportional to the observed light intensity.

Unburned hydrocarbon levels were measured with a flame ionization detector (FID) that uses a metal collector charged with a high DC voltage to detect ions formed when hydrocarbons in the sample are burned; the sample's HC concentration is directly proportional to the resulting current. Carbon monoxide and carbon dioxide were measured with an infrared detector that determines the concentration of carbon oxides by monitoring the absorption of infrared beams of a given wavelength. Measurements with all three of these gas analyzer modules have a reproducibility of 0.5% over the instrument's full measurement range.

The particle mass per cubic meter of exhaust gas was measured with an AVL Micro Soot Sensor. This device uses photoacoustics to detect particle mass flow; the basic setup of the measuring unit is shown in Figure 3.1a. In this system, particles are exposed to modulated light. Upon heating, the particles expand, generating a sound wave that can be detected using microphones. The signal increases in proportion to the concentration of particles in the exhaust sample. The instrument's measuring range is 0.001-50 mg/m^3. To prevent condensation, the exhaust gas must be diluted with the integrated conditioning unit [42].

The particle size distribution in the exhaust was measured with a Cambustion DMS500 unit capable of detecting particles between 5 nm and 2.5 μm in diameter. In this instrument, the gas sample is passed through a corona charger that gives each incoming particle a positive charge proportional to its surface area. The charged particles then enter a classifier column (Figure 3.1b) where they are separated according to their charge and aerodynamic drag. An electronic amplifier converts the resulting currents into data on particle numbers and sizes. The dilution factor was

kept constant during the measurements because particle size measurements depend strongly on dilution [43]. Samples for both the Micro Soot Sensor and the DMS500 were taken at the exhaust tailpipe.

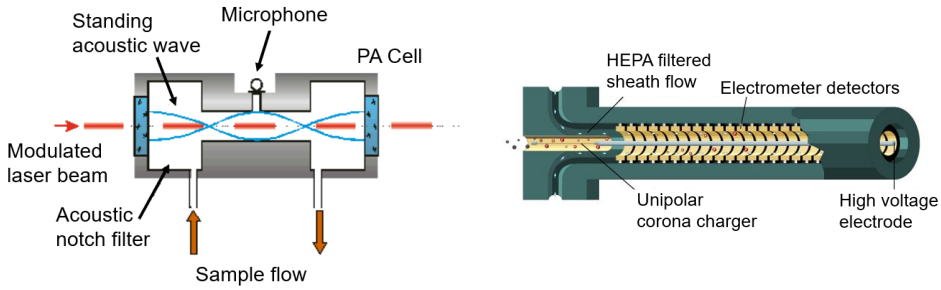

Figure 3.1: Schematic depictions of (a) a resonant cell in the MicroSoot instrument, adapted from [42];(b) the DMS500 instrument [43].

3.2.2 Combustion analysis

Indicated thermal efficiency

The *indicated thermal efficiency* η_t describes is the ratio of produced work and the work supplied to the system:

$$\eta_t = \frac{imep \cdot V_d}{m_{Fuel} \cdot LHV} \tag{1}$$

Here, *imep* is the indicated mean effective pressure, V_d is the displacement volume of the engine, *m(Fuel)* is the mass flow of fuel and *LHV* is the fuel's lower heating value. The *imep* is calculated from the sum of the compression and expansion stroke work divided by the displacement volume and so is a linear function of the cylinder pressure [44].

Coefficient of variation

Cycle-to-cycle variation can be assessed in terms of the *coefficient of variation (COV)* in *imep*, which can be computed using equation [44]:

$$COV_{imep} = \frac{\sigma_{imep}}{imep \cdot 100} \tag{2}$$

The COV increases as the stability of combustion decreases. Combustion is acceptably stable when the COV is below 3%.

Heat release analysis

The heat released at each crank angle can be derived from cylinder pressure traces and knowledge of the cylinder volume. The data acquisition system software OSIRIS records cylinder pressure traces, enabling extrapolation of the rate of heat release. There are various ways of calculating the heat release, all of which are based on the first law of thermodynamics, which states that the change in the heat transfer rate, *dQ/dt*, equals the internal energy *dU/dt* plus the work done, *dW/dt*, in a quasi-static system. This is expressed in equation 3:

$$\frac{dQ}{dt} = \frac{dU}{dt} + \frac{dW}{dt} \tag{3}$$

Assuming that the gases in the combustion chamber are ideal, the internal energy and the work transfer can be calculated as follows:

$$\frac{dU}{dt} = mc_v dT \tag{4}$$

$$\frac{dW}{dt} = pdV \tag{5}$$

Here m is the mass flow into the system, c_v is the heat capacity at a specific volume, and p is the pressure. Combining equation 3–5 with the ideal gas law $pV=mRT$, where R is the ideal gas constant, T can be eliminated. This yields the following expression:

$$\frac{dQ}{dt} = \frac{1}{(\kappa - 1)} V \frac{dp}{dt} + \frac{\kappa}{(\kappa - 1)} p \frac{dV}{dt} \tag{6}$$

The polytrophic exponent $\kappa = (c_v+R)/c_v$ defines the rate of specific heat at a given pressure and volume for the chosen working fluid. The polytrophic coefficient varies during the combustion process. To simplify the calculations, it is assumed to be between 1.3 and 1.35 for Diesel [44].

3.2.3 Statistical data evaluation

To ensure consistent initial conditions, all engine experiments began by operating the engine using Diesel fuel at the B50 load point for at least 30 minutes. The fuel scale and filter were then emptied, and the engine was run for at least 30 minutes with the fuel blend to be studied in order to eliminate residual Diesel fuel from the line. To maintain a constant mass flow, the injection duration was allowed to vary; in general, it remained within $\pm$ 0.003 CAD of the specified value. The EGR rate was set with an accuracy of $\pm$ 0.3%. Table 3.4 summarizes the mean values, standard deviations and the 95% confidence intervals of engine performance metrics and emissions levels observed using the reference Diesel fuel.

Load points were run in the same order for each fuel type. The B50 load point was used as a reference and the standard deviations of the performance and emissions variables at this load

Table 3.4: Rigstability testing

		Mean	**Standard deviation**	**Confidence intervall 95%**
	Unit	μ	σ	$\mu \pm$
Performance				
Torque	Nm	160.20	1.13	0.51
IMEP	bar	10.96	0.06	0.04
FuelConvEff	%	40.74	0.36	0.17
Emission				
Specific NOx	g/kWh	6.52	0.38	0.17
Specific HC	g/kWh	0.09	0.01	0.00
Specific CO	g/kWh	0.31	0.01	0.01
Specific Soot	g/kWh	$7.87 \cdot 10^3$	$8.64 \cdot 10^4$	$5.35 \cdot 10^4$
Particle Number		$9.88 \cdot 10^6$	$1.11 \cdot 10^6$	$7.24 \cdot 10^5$

point for each fuel are given in Paper I. In addition, the carbon balance was calculated based on the relation of the carbon content of the injected fuel and the measured exhaust emissions. During the stability tests, 97% of the injected carbon was converted into exhaust emissions. The engine functions as a closed system, so the number of incoming and outgoing carbon atoms should be equal in principle. Figure 3.2 shows the carbon conversion efficiencies of the different fuels for the four load points. The maximum loss of carbon from the system was 6%; this apparent loss could be due to the assumptions made when calculating the carbon balance and the inherent error of the measurement techniques. The quantity of incoming carbon is estimated as the product of the carbon content of the fuels in the blend (as given in Tables 2.1 and 3.1) and the fuel mass flow rate. The carbon contents for Diesel, RME and HVO are averages provides by the manufacturers, and may vary from batch to batch. Additionally, there is an error of 1% in the recorded fuel mass balance. The carbon leaving the system mainly consists of CO_2 and small amounts of HC, CO, and soot particles. The accuracy of FID-based HC measurements depends on the chemical composition of the carbon in the sample [45]. Furthermore, it is assumed that all soot particles consist exclusively of carbon. Although the measurement instruments were calibrated before every set of fuel tests, small uncertainties in the calibration gases and measurement instruments could give rise to aberrant measurements. Finally, the influence of oil particles in the exhaust and oil dilution are unknown.

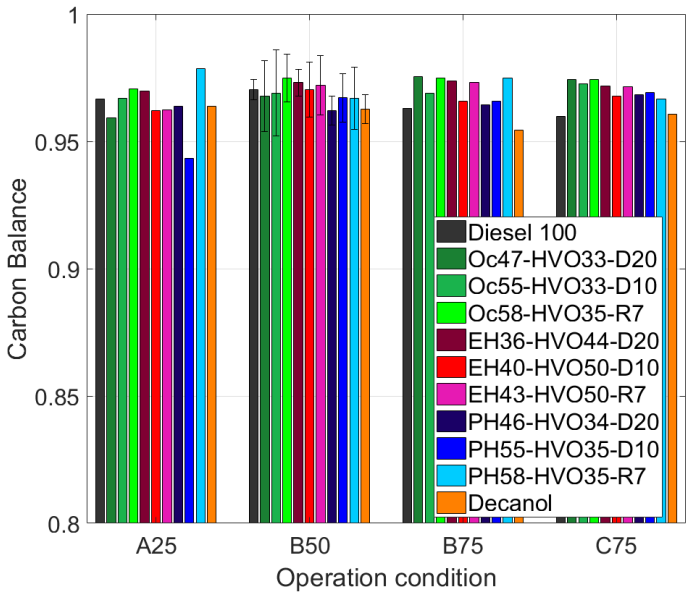

Figure 3.2: Carbon balance for heavy duty engine tests

3.3 High-pressure/high-temperature chamber

Experiments were performed in an optically accessible high-pressure/high-temperature chamber with a constant volume of 2 L. A 4-stage compressor continuously delivered compressed air at pressures of up to 10 MPa. Electric heaters were used to heat the air (to up to 900 K) before it entered the chamber. The inlet air flow velocity was 0.1 m/s. Fuel was injected at the bottom of the chamber using a Scania XPI injector with an axially symmetric single-orifice nozzle, 190 μm in diameter. The fuel was supplied via a common rail system connected to a Scania XPI high pressure pump. A more detailed description of the chamber and cameras is presented in earlier publications [46, 47]. Combusting and non-combusting cases were studied at injection pressures of 180 MPa and 120 MPa, respectively, with a gas density of 26 kg/m^3. For non-combusting conditions, the temperature in the spray chamber was set to 623 K (350°C) and the ambient pressure to 4.59 MPa. For combusting conditions, the temperature was set to 823 K (550°C) and pressure to 6.04 MPa. These settings approximate those generated in a heavy duty CI engine operating under low load. At least 30 injection events were studied for each set of experimental conditions, and the subsequent data analysis was based on results averaged over these events. Table 3.5 summarizes the experimental conditions used in this campaign.

Table 3.5: Experimental conditions used in the high-pressure/high-temperature chamber

		Non-combusting	Combusting
Injection pressure	MPa	120, 180	
Ambient temperature	K ($°C$)	623 (350)	832 (550)
Ambient pressure	MPa	4.59	6.04
Ambient density	Kg/m^3	26	
Injection pulse duration	ms	1.7	3
Frequency of injections	Hz	0.1	
Number of injections	-	30	

3.3.1 Optical setup

Various spray characteristics were measured using different optical methods. Shadowgraph imaging was used to determine the liquid and vapor phase penetration of non-combusting sprays. As shown in Figure 3.3, a diffuse screen was placed in front of halogen lamps to create diffuse background illumination. The diffusor plate was an iced plate when measuring liquid penetration,

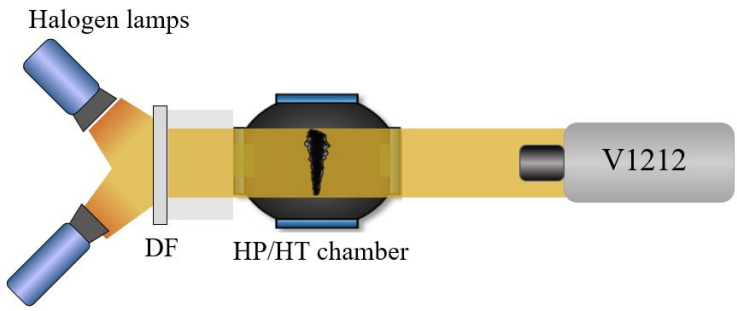

Figure 3.3: Optical setup for liquid and vapor phase imaging. The diffusor plate (DF) was an iced plate when measuring liquid phase penetration detection and a striped plate when measuring vapor penetration.

but was replaced with a striped plate when measuring vapor phase penetration. The method of exploiting the recurring contrast between light and dark stripes to visualizes vapor penetration is known as the background grid distortion method. Schardin [48] introduced this method as 'schlieren method no. 2' and it was later adapted for vapor phase imaging by Ochoterena [49]. The optical setup for capturing light extinction, flame luminosity and OH*chemiluminescence is described in Paper II.

3.3.2 Image analysis

Cone angle calculations

The spray cone angle θ was calculated using the equation introduced by Naber and Siebers [50]:

$$\frac{\theta}{2} = tan^{-1} \cdot \frac{A_{P,\frac{L}{2}}}{(\frac{L}{2})^2} \tag{7}$$

Here, $A_{(p,L/2)}$ is the spray area of the upstream half of the spray and L is the spray penetration length for the liquid phase, defined as the distance between the nozzle and the tip of the liquid fuel jet. Figure 3.4 illustrates the quantities used to calculate the spray angle. The black spray boundary is obtained by defining a threshold level that is used to convert the greyscale spray images into binary images. This is further explained in Paper II and in the publications of Du et al. [47, 51].

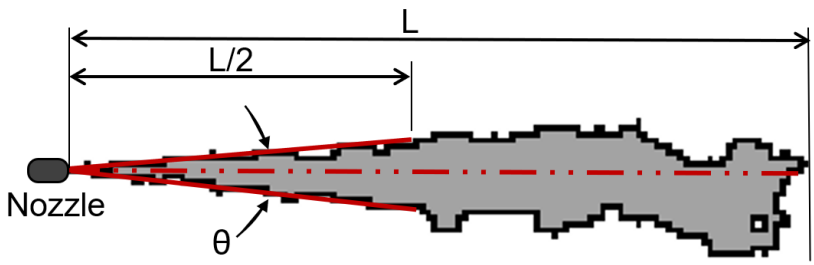

Figure 3.4: Spray cone angle calculation (adapted from [50])

Lift-off length

The lift-off length is commonly defined as distance between the nozzle tip and the mean flame location, which was determined by analyzing OH*chemiluminescence images. Figure 3.5a shows the intensity profile along the fuel jet centerline. The threshold used to delineate the boundary of the flame, as shown in Figure 3.5b, was set to a value corresponding to around 50% of the intensity at the 'knee' of the intensity profile. This method is an adaptation of that proposed by Siebers and Higgins [52].

Ignition delay

The ignition delay is the time between the start of fuel injection and the start of detectable combustion. During this time, the initial fuel air mixture is formed. Physical processes governing the length of the ignition delay include fuel-air mixing, spray breakup and droplet formation, vaporization of the heated fuel and the formation of a combustible vapor air mixture. OH*chemiluminescence imagining can be used to visualize the formation of OH*radicals during

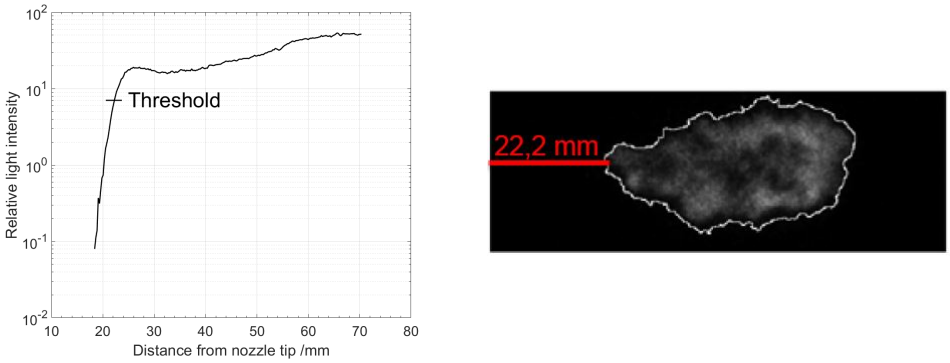

Figure 3.5: Diesel spray OH* chemiluminescence at 550°C, 4.6 MPa, p_{inj} = 120 MPa, 3.6 ms ASOI: (a) Intensity profile from averaged images, (b) OH* chemiluminescence image showing the flame boundary.

high temperature reactions, which begin at the moment of ignition (it should be noted that ignition may occur in several places simultaneously). The ignition delay is thus equal to the length of time between the fuel entering the chamber and the first appearance of OH*chemiluminescence. Longer ignition delays enable the formation of more homogeneous fuel-air mixtures.

4 Results

4.1 Summary of Paper I

The performance and emissions of a heavy duty CI engine was investigated when using various long-chain alcohol blends and conventional fossil Diesel fuel. The engine's performance was measured in terms of its indicated thermal efficiency, the COV in IMEP, and the rate of heat release. The COV was below 1.5% for all fuels at all loads, indicating that stable combustion was achieved in all cases. Additionally, all fuels yielded similar thermal efficiencies at the A25, B75 and C75 load points. However, at the reference B50 load point, the blends' thermal efficiencies exceeded that of Diesel. The blends' heating values were slightly lower than those of Diesel, so the indicated mean effective pressure when using the blends was between 3.5% and 6% lower than that when using Diesel, depending on the blend and load case. In addition, the blends yielded slightly higher specific fuel consumption values than Diesel. The rate of heat release was similar for all tested fuels. The CA50 (i.e. the crank angle degree at which 50% of the fuel is burned) advanced with the oxygen content of the fuel at the A25, B50, and B75 load points. However, the combustion duration was independent of the oxygen content under high load conditions (i.e. at the C75 load point). The exhaust gas temperature observed when using the blends was on average 24 K lower than that when using Diesel. The NOx and HC emissions generated when using the blends did not differ significantly from those observed when using Diesel, but the CO emissions when using the blends were significantly lower. However, reducing the content of fossil Diesel (from 20% to 10%) in the blends did not cause a linear decrease in emissions. The use of blends reduced the soot mass by up to 62% at the high load point (C75). These results agree with the conclusions of previous studies on long-chain alcohols, which concluded that they significantly reduced soot emissions because of the alcohols' higher heat of evaporation and the greater soot oxidation due to the oxygen content of the fuel. Blends containing RME rather than fossil Diesel yielded the lowest particle mass emissions because they contain no aromatic compounds, which are key precursors for soot formation. On average, the use of RME in place of Diesel reduced soot mass by 47%. However, the blends had a significantly higher number of particles with diameters below 23 nm. The particle size distribution for the blends was dominated by nucleation mode particles, which could be a challenge for aftertreatment systems. As stated previously, agglomeration mode particles typically account for at least 90% of the total mass of emitted particulate matter Kittelson [53]. The particles generated by Diesel combustion tend to form agglomerates, so the total particle mass for Diesel was higher and the total particle number was lower. Soot oxidation and NOx formation both strongly depend on

the temperature in the combustion chamber. High temperatures promote soot oxidation but lead to higher NOx emissions; this behavior is known as the soot-NOx trade off (e.g. [7, 27, 54]). The observed reduction in soot emissions when using blended fuels may be primarily due to reductions in the rates of the initial steps of soot formation because no significant increases in NOx emissions were observed. The alcohols' higher heat of evaporation may also help reduce local temperatures in the reaction zone, which could reduce soot particle formation.

4.2 Summary of Paper II

In an optically accessible high-pressure/high temperature chamber under non-combusting (623 K, 4.59 MPa) and combusting conditions (823 K, 6.04 MPa), spray characteristics of fuel blends based on the long-chain alcohol 2-ethylhexanol, HVO, and fossil Diesel or RME were compared to those of HVO and Diesel. Injection pressures of 120 MPa and 180 MPa were used at a stable ambient gas density of 26 kg/m^3. Several optical imaging techniques were used to obtain information about the spray characteristics. The liquid and vapor penetration length were captured by means of shadow imaging under non-combusting conditions. Under combusting conditions, time-resolved two-dimensional light extinction imaging was performed. The use of monochromatic laser light made it possible to acquire direct quantitative measurements even in strongly luminescent flames. Flame luminosity and OH* chemiluminescence images were acquired simultaneously to the light extinction images.

Under non-combusting conditions, liquid penetration lengths for the blends and HVO were found to be higher than that for Diesel, but all of the tested fuels had similar vapor penetration lengths. The higher liquid penetration lengths of the blends may be due to the higher latent heat of evaporation of 2-ethylhexanol, which means that more energy is required to induce a transition from the liquid to the vapor phase.

The fuels' ignition delay times were compared under combusting conditions. Despite having similar CN values to Diesel, the alcohols had longer ignition delays. Moreover, HVO and Diesel had similar ignition delays even though the CN of HVO is appreciably higher than that of Diesel. The lift-off length (i.e. the distance between the nozzle and the location of autoignition) was determined based on the detection of OH* radicals, and was similar for HVO and Diesel. The similarity of the spray characteristics of Diesel and HVO is consistent with previous literature reports. The blends' lift-off lengths were higher than that of Diesel. Longer lift-off lengths and ignition delays provide more time for air-fuel mixing before ignition, resulting in more homogeneous combustion. The longer ignition delays and lift-off lengths observed for the blends can be attributed to the alcohols' higher latent heats of evaporation. Due to the lack of soot precursors in the EHR7 blend and its shorter residence time, soot formation was suppressed. Consequently, this fuel produced the lowest soot volume fraction.

The optical measurements confirmed the results of the engine tests and provided valuable information about the spray characteristics. In particular, they revealed that both the oxygen content of a fuel and the latent heat of vaporization of its components have significant effects on its spray characteristics and thus the emissions it generates when burned.

5 Outlook

Long-chain alcohols were blended with HVO and Diesel or RME to evaluate the suitability of such mixtures as future transportation fuels. Blends were used instead of neat components to overcome the disadvantages of using fuel components in neat form and to obtain blends whose properties resemble those of Diesel, enabling their use as drop-in fuels for existing Diesel engines.

Experiments were conducted in a heavy duty compression ignition engine to compare the performance and emissions achieved when using different blends to those achieved with neat Diesel. Additionally, the spray characteristics of selected blends were investigated in a high-pressure/high-temperature chamber. Overall, the tested blends of long-chain alcohols, HVO, and RME or Diesel were found to be suitable for use in heavy duty CI engines. However, in the long term, it will be necessary to develop fuels consisting exclusively of renewable substances. Therefore, future studies should focus on Diesel-free fuel blends and the design of single-component fuels. A promising candidate fuel of this type is polyoxymethylene dimethyl ether (OME), which can be produced sustainably and burned in neat form in CI engines.

Both the engine and optical experiments indicated that particle emissions decrease as the alcohol content of the fuel increases due to both the greater oxygen content of the fuel and the alcohols' higher latent heats of evaporation. Previous publications have discussed the effect of oxygenation on engine out soot emissions but there has been less emphasis on the role of the fuel's latent heat of evaporation. Consequently, the effects of this variable warrant further investigation.

Abbreviations

A_P	Projected area of the spray jet
COV	Coefficient of variation
D	Diesel
Dec	n-Decanol
EH	2-Ethylhexanol
HVO	Hydrotreated vegetable oil
imep	Indicated mean effective pressure
L	Liquid penetration length
LHV	Lower heating value
Oc	n-Octanol
PH	2-Propylheptanol
PMP	Particle Measurement Programme
LHV	Lower Heating value
RoHR	Rate of heat release
RME	Rapeseed methyl ester
V_d	Displacement volume

References

[1] International Energy Agency (IEA), "CO_2 emissions from fuel combustion," pp. 1–162, 2017.

[2] A. Sydbom, A. Blomberg, S. Parnia, N. Stenfors, T. Sandström, and S. Dahlén, "Health effects of diesel exhaust emissions," *European Respiratory Journal*, vol. 17, no. 4, pp. 733–46, 2001.

[3] DieselNet, "Emission standards - Summary of worldwide engine and vehicle emission standards," 2018. [Online]. Available: https://www.dieselnet.com/standards/

[4] B. Giechaskiel, R. Chirico, P. F. DeCarlo, M. Clairotte, T. Adam, G. Martini, M. F. Heringa, R. Richter, A. S. H. Prevot, U. Baltensperger, and C. Astorga, "Evaluation of the particle measurement programme (PMP) protocol to remove the vehicles' exhaust aerosol volatile phase," *Science of the Total Environment*, vol. 408, no. 21, pp. 5106–5116, 2010.

[5] J. Campos-Fernández, J. M. Arnal, J. Gómez, and M. P. Dorado, "A comparison of performance of higher alcohols/diesel fuel blends in a diesel engine," *Applied Energy*, vol. 95, pp. 267–275, 2012.

[6] H. S. Hess, J. Szybist, A. L. Boehman, P. J. A. Tijm, and F. J. Waller, "Impact Of Oxygenated Fuel On Diesel Engine Performance And Emissions," *Proceedings of NHTC'01, 35th National Heat Transfer Conference*, vol. NHTC01-114, pp. 1–11, 2001.

[7] B. Heuser, F. Kremer, S. Pischinger, J. Julis, and W. Leitner, "Optimization of diesel combustion and emissions with newly derived biogenic alcohols," *SAE Technical Paper 2013-01-2690*, vol. 11, 2013.

[8] J. Manin, S. Skeen, L. Pickett, E. Kurtz, and J. E. Anderson, "Effects of Oxygenated Fuels on Combustion and Soot Formation/Oxidation Processes," *SAE International Journal of Fuels and Lubricants 2014-01-2657*, vol. 7, no. 3, pp. 704–717, 2014.

[9] European Committee for Standardization, "EN 590: Automotive fuels - Diesel - Requirements and test methods, European Committee for Standardization," 2009, ref. No. EN 590:2009.

[10] Neste, "Safety data sheet: Neste Diesel fuel, sulphur free," 2017.

[11] Sigma-Aldrich, "1-Octanol, 95446," *Safety Data Sheet*, 2015.

[12] Perstorp BioProducts AB, "2-Propylheptanol," *Safety data sheet according to 1907/2006/EC, Article 31*, pp. 1–12, 2015.

[13] Neste Oil, "Hydrotreated vegetable oil (HVO)-premium renewable biofuel for diesel engines," *Safety Data Sheet*, 2014.

[14] Perstorp BioProducts AB, "RME - Perstorp BXN," *Safety Data Sheet according to 1907/2006/EC, Article 31*, 2016.

[15] N. Yoshimura and M. Tamura, "Process for producing normal-octanol," 1981, uS Patent 4417079A.

[16] M. K. Akhtar, H. Dandapani, K. Thiel, and P. R. Jones, "Microbial production of 1-octanol: A naturally excreted biofuel with diesel-like properties," *Metabolic Engineering Communications*, vol. 2, pp. 1–5, 2015.

[17] T. Hamilton-Kemp, M. Newman, R. Collins, H. Elgaali, K. Yu, and D. Archbold, "Production of the long-chain alcohols octanol, decanol, and dodecanol by Escherichia coli," *Current Microbiology*, vol. 51, no. 2, pp. 82–86, 2005.

[18] J. Julis and W. Leitner, "Synthesis of 1-octanol and 1,1-dioctyl ether from biomass-derived platform chemicals," *Angewandte Chemie - International Edition*, vol. 51, no. 34, pp. 8615–8619, 2012.

[19] G. Kessen, B. Cornils, W. Gick, E. Wiebus, J. Hibbel, H. Bach, and W. Zgorzelski, "Process for the production of 2-ethyl-hexanol," 1985, US Patent 5227544.

[20] R. Miller and G. Bennett, "Producing 2-Ethylhexanol by the Guerbet Reaction," *Industrial and Engineering Chemistry*, vol. 51(1), pp. 33–36, 1961.

[21] D. Rakopoulos, C. Rakopoulos, E. Kakaras, and E. Giakoumis, "Effects of ethanol–diesel fuel blends on the performance and exhaust emissions of heavy duty DI diesel engine," *Energy Conversion and Management*, vol. 49, no. 11, pp. 3155–3162, 2008.

[22] Swedish Energy Agency, "Energy in Sweden-Fact and Figures 2018," 2018.

[23] M. Johansson, M. Ehleskog, S. Gjirja, and I. Denbratt, "Effects of varying engine settings on combustion parameters, emissions, soot and temperature distributions in low temperature combustion of fischer-tropsch and swedish diesel fuels," *SAE Technical Paper 2009-01-2787*, vol. 4970, 2009.

[24] K. J. Ptasinski, *Efficiency of Biomass Energy - An Exergy Approach to Biofuels, Power, and Biorefineries*. John Wiley & Sons, Inc, 2016.

[25] A. Tsolakis, A. Megaritis, M. L. Wyszynski, and K. Theinnoi, "Engine performance and emissions of a diesel engine operating on diesel-RME (rapeseed methyl ester) blends with EGR (exhaust gas recirculation)," *Energy*, vol. 32, no. 11, pp. 2072–2080, 2007.

[26] A. Atmanli, "Effects of a cetane improver on fuel properties and engine characteristics of a diesel engine fueled with the blends of diesel , hazelnut oil and higher carbon alcohol," *Fuel*, vol. 172, pp. 209–217, 2016.

[27] A. Janssen, M. Muether, S. Pischinger, A. Kolbeck, and M. Lamping, "Tailor-Made Fuels: The Potential of Oxygen Content in Fuels for Advanced Diesel Combustion Systems," *SAE International 2009-01-2765*, 2009.

[28] C. Weiskirch, M. Kaack, I. Blei, and P. Eilts, "Alternative Fuels for Alternative and Conventional Diesel Combustion Systems," *SAE Technical Paper 2008-01-2507*, 2008.

[29] T. Zhang, K. Munch, and I. Denbratt, "An Experimental Study on the Use of Butanol or Octanol Blends in a Heavy Duty Diesel Engine," *SAE International Journal of Fuels and Lubricants 2015-24-2491*, vol. 8, no. 3, 2015.

[30] K. Weidmann and H. Menrad, "Fleet Test, Performance and Emissions of Diesel Engines Using Different Alcohol-Diesel fuel Blends," *SAE Technical Paper 841331*, 1984.

[31] J. Campos-Fernández, J. M. Arnal, J. Gomez, N. Lacalle, and M. P. Dorado, "Performance tests of a diesel engine fueled with pentanol/diesel fuel blends," *Fuel*, vol. 107, pp. 866–872, 2013.

[32] D. Rakopoulos, C. Rakopoulos, R. Papagiannakis, and D. Kyritsis, "Combustion heat release analysis of ethanol or n-butanol diesel fuel blends in heavy-duty DI diesel engine," *Fuel*, vol. 90, no. 5, pp. 1855–1867, may 2011.

[33] R. Swamy, T. Chandrashekar, N. Banapurmath, and S. Khandal, "Impact of Diesel-butanol Blends on Performance and Emission of Diesel Engine," *Oil and Gas Research*, vol. 1, no. 1, pp. 1–7, 2015.

[34] A. García, J. Monsalve-Serrano, B. Heuser, M. Jakob, F. Kremer, and S. Pischinger, "Influence of fuel properties on fundamental spray characteristics and soot emissions using different tailor-made fuels from biomass," *Energy Conversion and Management*, vol. 108, pp. 243–254, 2016.

[35] H. Aatola, M. Larmi, T. Sarjovaara, and S. Mikkonen, "Hydrotreated Vegetable Oil (HVO) as a Renewable Diesel Fuel: Trade-off between NOx, Particulate Emission, and Fuel Consumption of a Heavy Duty Engine," *SAE Technical Paper 2008-01-2500*, 2008.

[36] T. Hartikka, M. Kuronen, and U. Kiiski, "Technical Performance of HVO (Hydrotreated Vegetable Oil) in Diesel Engines," *SAE Technical Paper 2012-01-1585*, 2012.

[37] M. Lapuerta, M. Villajos, J. R. Agudelo, and A. L. Boehman, "Key properties and blending strategies of hydrotreated vegetable oil as biofuel for diesel engines," *Fuel Processing Technology*, vol. 92, no. 12, pp. 2406–2411, 2011.

[38] J. E. Dec, "A conceptual model of DI diesel combustion based on laser-sheet imaging," *SAE Technical Paper 970873*, 1997.

[39] H. Kosaka, T. Aizawa, and T. Kamimoto, "Two-dimensional imaging of ignition and soot formation processes in a diesel flame," *International Journal of Engine Research*, vol. 6, pp. 21–42, 2005.

[40] D. B. Kittelson, "Engines and nanoparticles: A review," *Journal of Aerosol Science*, vol. 29, no. 5-6, pp. 575–588, 1998.

[41] D. Kittelson and M. Kraft, "Particle Formation and Models in Internal Combustion Engines," in *Encyclopedia of Automotive Engineering*. Wiley, 2014, ch. 8.

[42] AVL List GmbH, "AVL Micro Soot Sensor: Operating Manual," List, 2013.

[43] Cambustion, "DMS500 Fast Particle Analyzer," 2018. [Online]. Available: https://www.cambustion.com/products/dms500

[44] J. B. Heywood, *Internal Combustion Engine Fundamentals*. McGrawHill, 1988.

[45] R. A. Morris and R. L. Chapman, "Flame Ionization Hydrocarbon Analyzer," *Journal of the Air Pollution Control Association*, vol. 11, no. 10, pp. 467–489, 1961.

[46] C. Du, M. Andersson, and S. Andersson, "Effects of Nozzle Geometry on the Characteristics of an Evaporating Diesel Spray," *SAE International Journal of Fuels and Lubricants*, vol. 9, no. 3, pp. 493–513, 2016.

[47] C. Du, S. Andersson, and M. Andersson, "Two-dimensional measurements of soot in a turbulent diffusion diesel flame: the effects of injection pressure, nozzle orifice diameter, and gas density," *Combustion Science and Technology*, vol. 190, no. 9, pp. 1659–1688, 2018.

[48] H. Schardin, "Die Schlierenverfahren und ihre Anwendungen," in *Ergebnisse der Exakten Naturwissenschaften*. Springer Berlin Heidelberg, 1942, pp. 303–439.

[49] R. Ochoterena, "High Speed Shadowgraph and Diffraction Based Imaging for Spray Characterisation and Combustion Studies," *SAE International 2009-24-0034*, 2009.

[50] J. Naber and D. L. Siebers, "Effects of Gas Density and Vaporization on Penetration and Dispersion of Diesel Sprays," *SAE Technical Paper 960034*, 1996.

[51] C. Du, M. Andersson, and S. Andersson, "The Influence of Ethanol Blending in Diesel fuel on the Spray and Spray Combustion Characteristics," *SAE International Journal of Fuels and Lubricants*, vol. 7, no. 3, pp. 823–832, 2014.

[52] D. L. Siebers and B. Higgins, "Flame Lift-Off on Direct-Injection Diesel Sprays Under Quiescent Conditions," *SAE Technical Paper 2001-01-0530*, 2001.

[53] D. B. Kittelson, "Recent Measurements of Nanoparticle Emissions from Engines," *Current Research on Diesel Exhaust Particles Japan Association of Aerosol Science and Technology*, 2001.

[54] M. Johansson, J. Yang, R. Ochoterena, S. Gjirja, and I. Denbratt, "NOx and soot emissions trends for RME, SME and PME fuels using engine and spray experiments in combination with simulations," *Fuel*, vol. 106, pp. 293–302, 2013.